Electronic Supplementary Information (ESI)

Kinetically-Enhanced Polysulfide Redox Reactions by Nb2O5 Nanocrystal for High-Rate Lithium–Sulfur Battery

Yingqing Tao, [a] Yanju Wei, [a] Yu Liu,* [a] Jitong Wang, [a] Wenming Qiao, [a, b] Licheng Ling, [a, b] and Donghui Long * [a, b]

[a] State Key Laboratory of Chemical Engineering, East China University of Science and Technology, Shanghai 200237, China

[b] Key Laboratory of Specially Functional Polymeric Materials and Related Technology, East China University of Science and Technology, Shanghai 200237, China.

* Corresponding author: longdh@mail.ecust.edu.cn; Tel./Fax: +86-21-64252924。

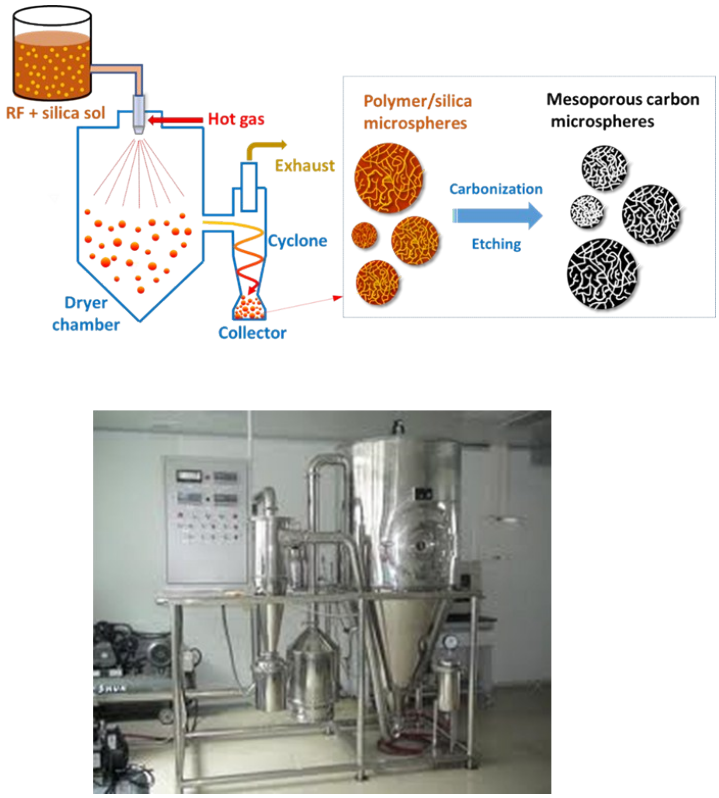

Figure S1. Formation process and instrument of the MCMs using the spray drying strategy.

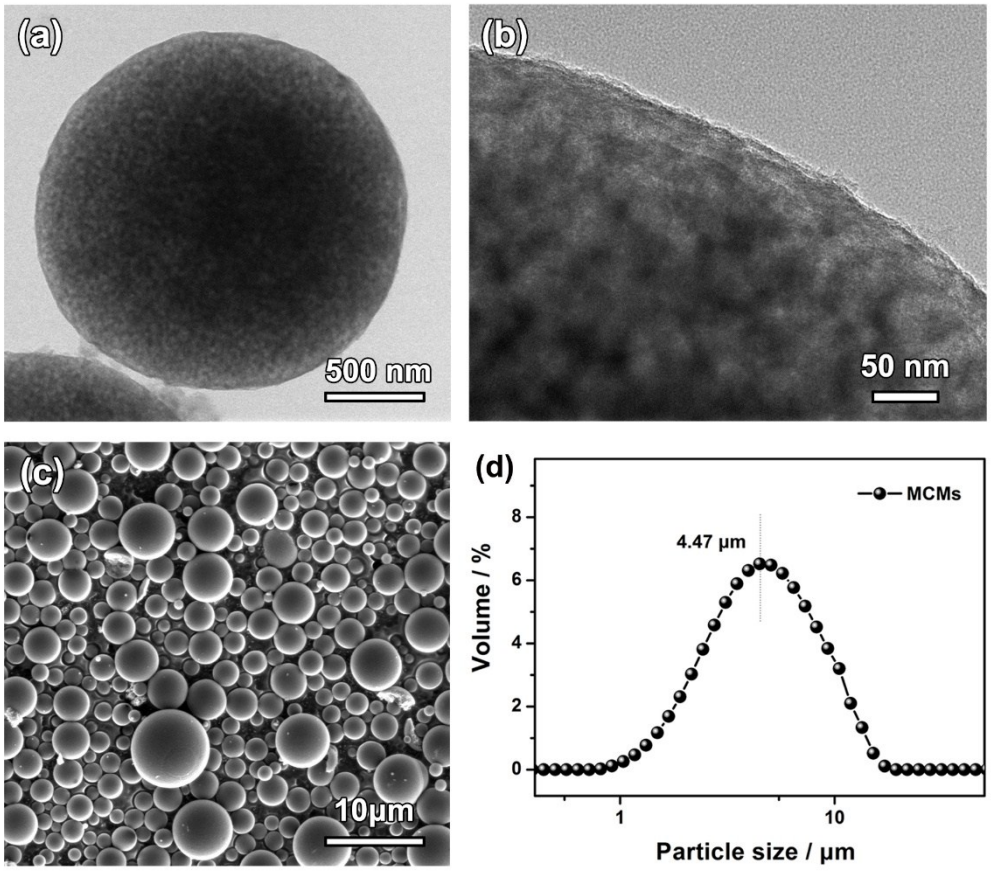

Figure S2. (a-b) TEM, (c) SEM images and (d) DSL particle size distribution of MCMs.

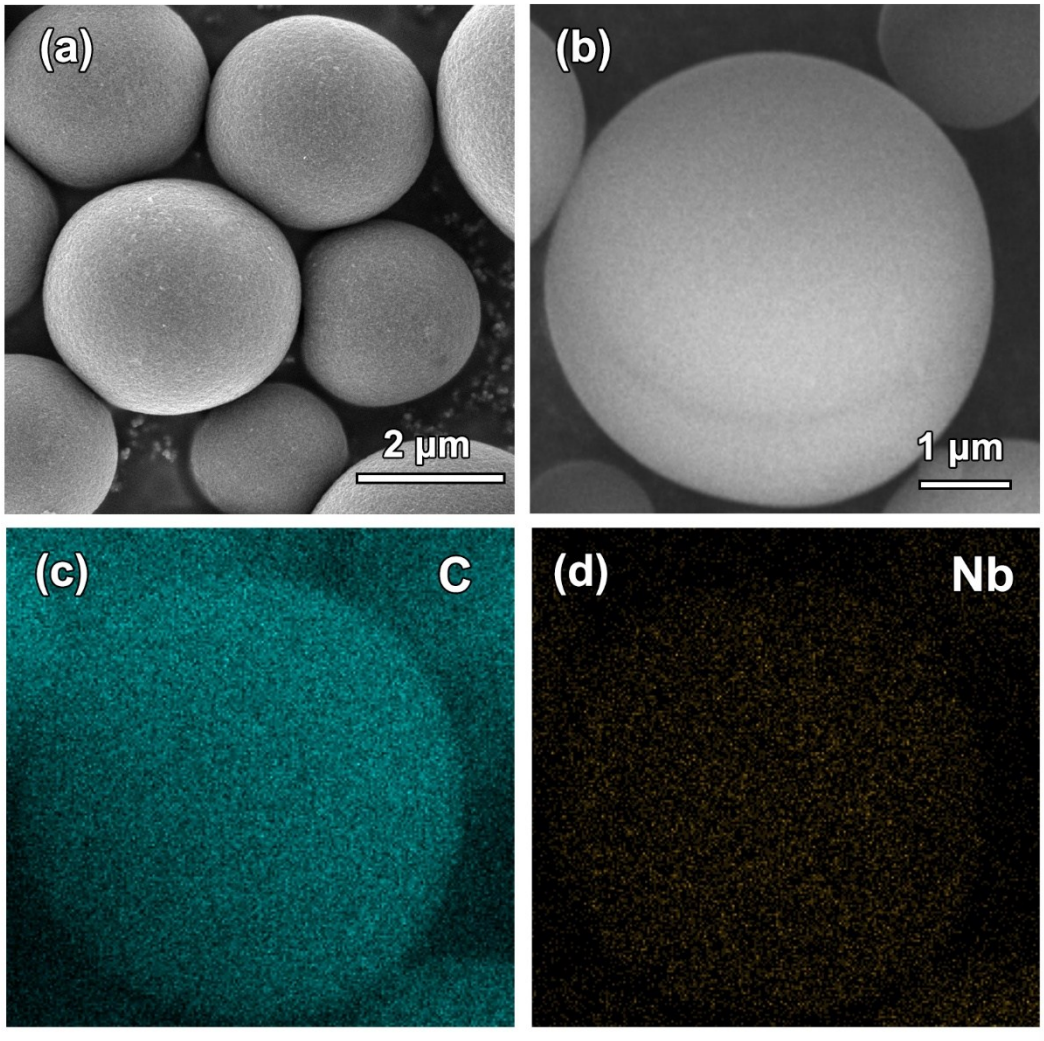

Figure S3. (a) SEM and (b-d) elemental mapping images of MCM/Nb_2O_5.

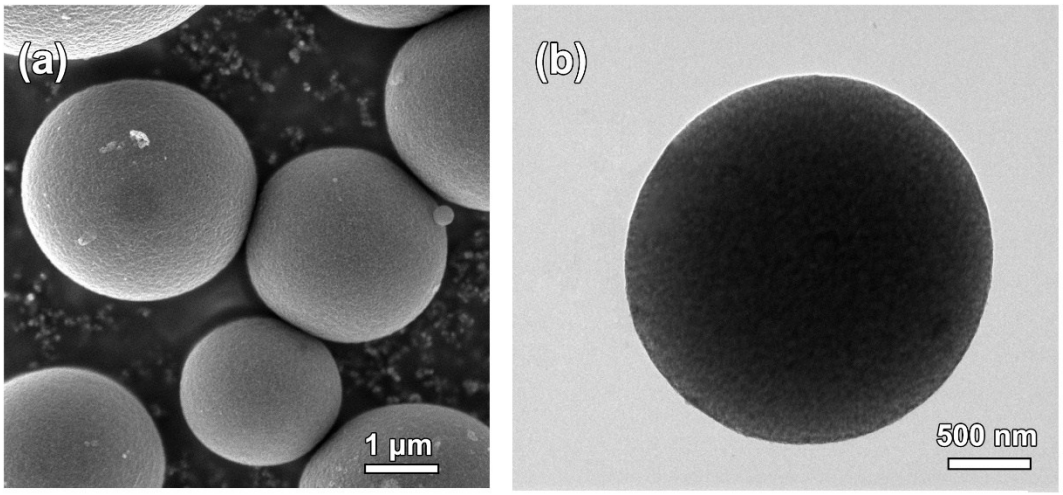

Figure S4. SEM and TEM images of MCM/Nb_2O_5/S composites.

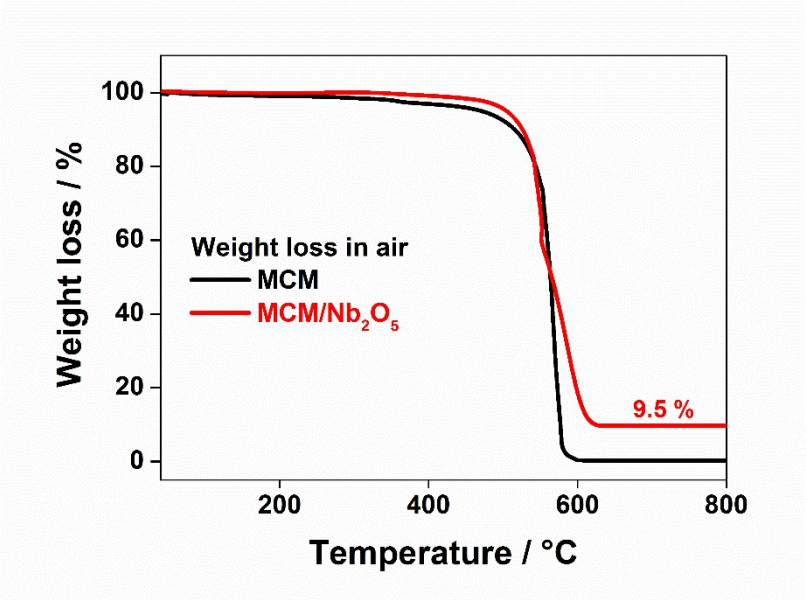

Figure S5. TGA curves of MCM/Nb_2O_5 in air.

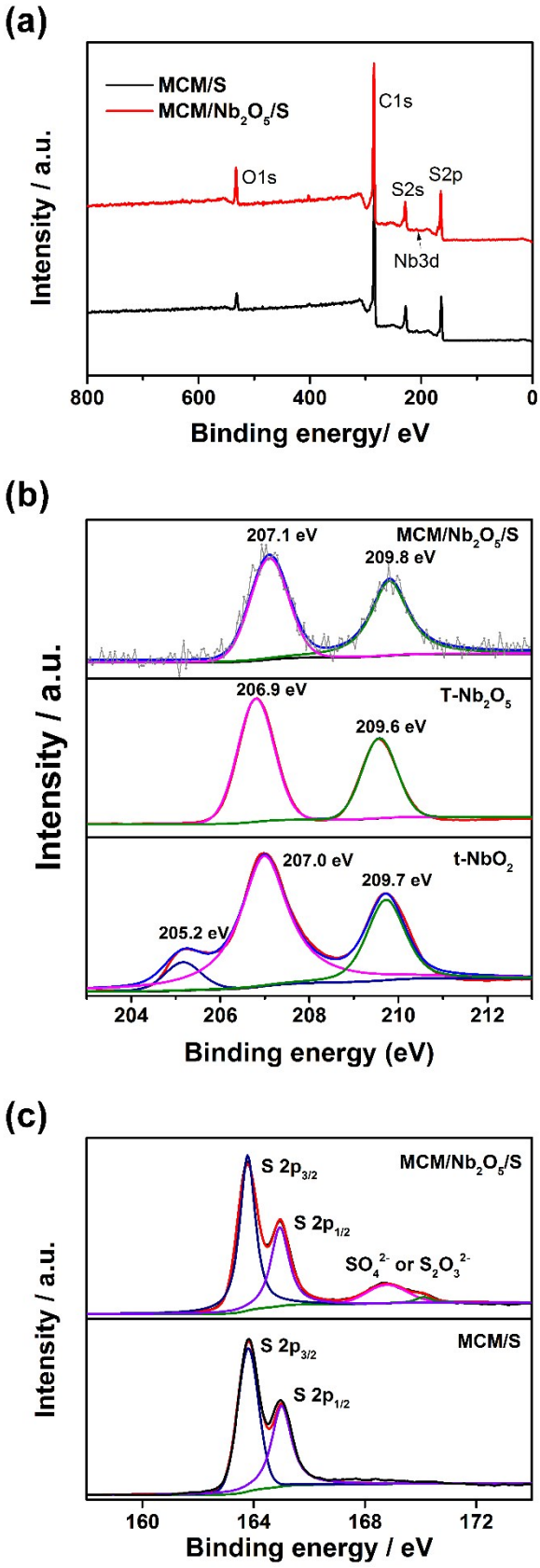

Figure S6. (a) XPS survey spectra of MCM/S and MCM/Nb_2O_5/S composite. (b)

High-resolution Nb3d XPS spectra of MCM/Nb_2O_5/S, orthorhombic (T-) Nb_2O_5 and tetragonal (t-) NbO_2. (c) High-resolution S2p XPS spectra of MCM/Nb_2O_5/S and MCM/S.

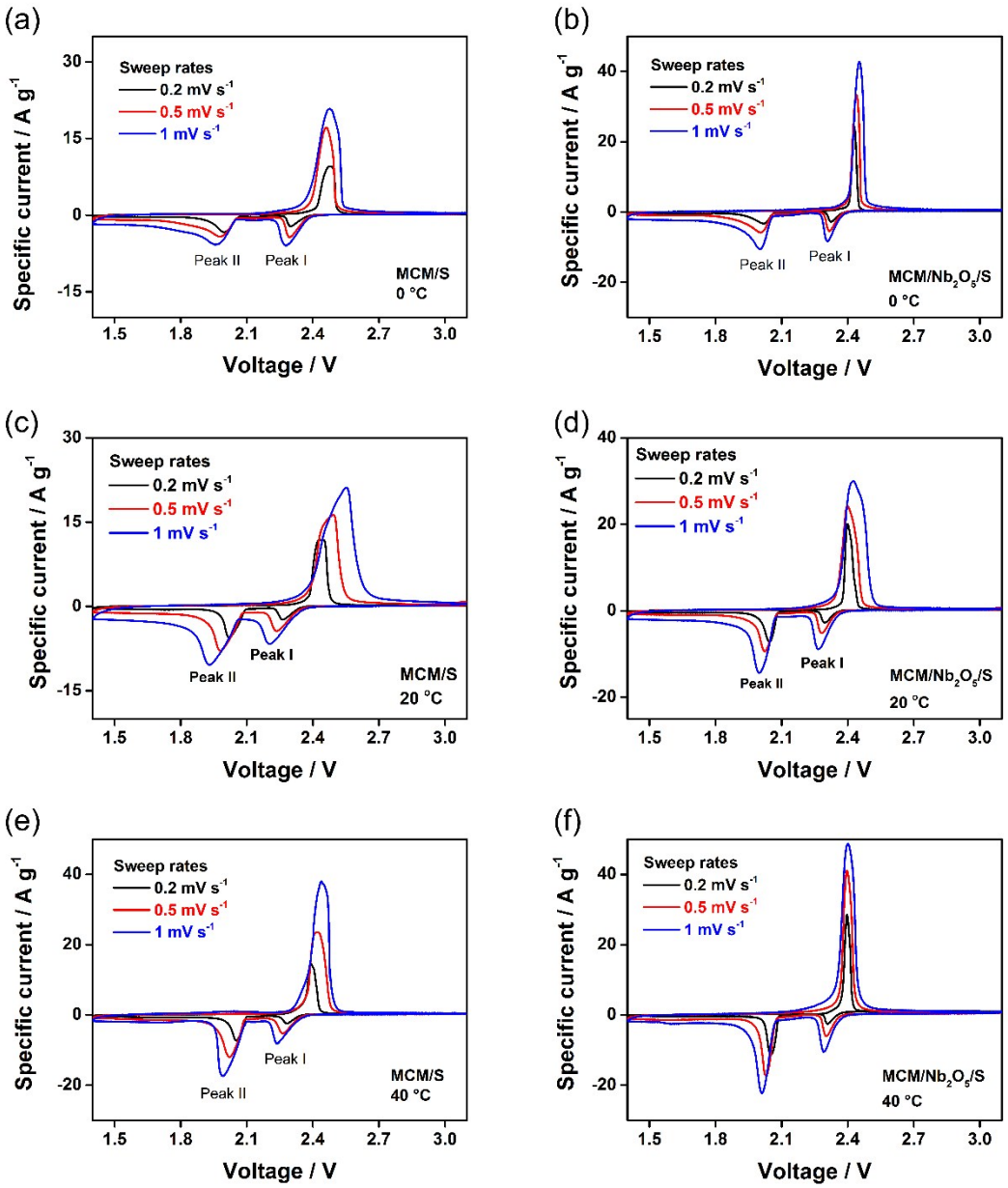

Figure S7. CV curves of MCM/Nb_2O_5/S ((a) 0 °C, (c) 20 °C, (e) 40 °C) and MCM/S ((b) 0 °C, (d) 20 °C, (f) 40 °C) cathodes under different sweep rates at different temperature.

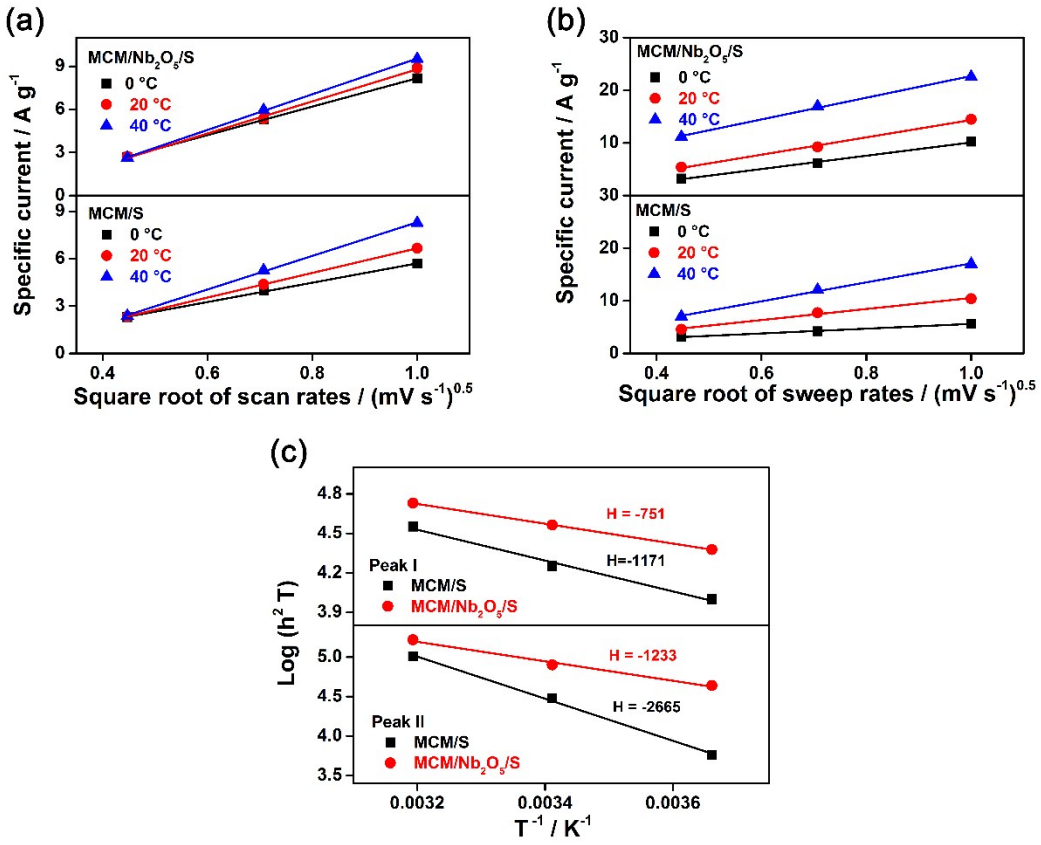

Figure S8. Relation of the pear current to the square rate of the scan rate: (a) peak I, (b) peak II. (c) Relation of the logarithm of (h^2 T) to inverse temperature.

CV tests were performed under different scan rates (0.2, 0.5 and 1 mV s^{-1}) at three temperatures (0 °C, 20 °C, 40 °C) as shown in Figure S7. Correspondingly, the activation energy of sulfur lithiation reactions over MCM/Nb_2O_5/S and MCM/S cathodes could be calculated as given in Figure S8.

As shown in Figure S8a and b, the cathodic peak currents are linear with the square rate of the scan rates at the same temperature. The slopes (h) of the curves in Figure S8a and b are positively correlated to the corresponding Li^+ diffusion coefficient according to the classical Randles Sevcik equation [1-2]:

$$i = 0.4463\ n\ F\ A\ C\ (n\ F\ v\ D / R\ T)^{1/2} \quad (1)$$

where i is the peak current, n is the number of electrons per reaction species, F is Faraday's constant (96485 C/mol), A is the active electrode area, R is the universal gas constant (8.314 J/mol K), C is the Li concentration, v is the scan rate, D is the Li^+ diffusion coefficient, T is the absolute temperature (K). The equation can be written in a more concise form:

$$i = (4.64 \times 10^6)\ n^{1.5}\ A\ D^{0.5}\ C\ v^{0.5}\ T^{-0.5} \quad (2)$$

The Li^+ diffusion coefficient (D) is expected to be proportional to the square of the slope (h) and the absolute temperature T. The n, A and C are considered as constants in one cathode system and the relationship could be simplified into:

$$h = r\ D^{0.5}\ T^{-0.5} \quad (3)$$

where r is considered as a constant for one cathode system.

The activation energy could be determined use the Arrhenius equation:

$$D = D_0\ e^{-Ea/kT} \quad (4)$$

Where D_0 is the preexponential factor, E_a is the activation energy, k is the Boltzmann's constant. The logarithm of the Li+ diffusion coefficient could be displayed as follow:

$$\text{Log } D = -E_a / kT + \text{Log } D_0 \quad (5)$$

The activation energy which could be estimated using eq (5) together with eq (3). Figure S8c. shows the logarithmic plot of (h^2 T) vs 1/T for the MCM/Nb_2O_5/S and MCM/S cathodes of peak I and peak II. It can be concluded that, at a temperature range of 273.15 - 313.15 K, the plot of log (h^2 T) vs inverse temperature has a good

linear relationship. For a qualitative comparison, the activation energy is negative correlated to the corresponding slope (H) of the curve in Figure S8c. Obviously, the slopes (H) of the cathodic peaks of MCM/Nb_2O_5/S cathode are larger than these of the MCM/S cathode, indicating a reduction in the reaction activation energies of sulfur lithiation. Also, the degree of slope change of peak II is more significant than that of peak I, in good agreement with the results of kinetic b values.

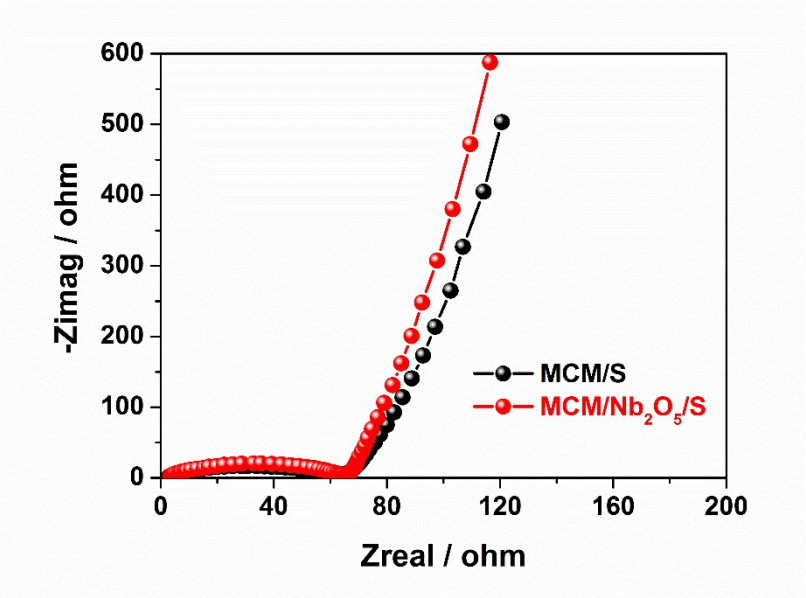

Figure S9. Nyquist plots of MCM/S and MCM/Nb_2O_5/S cathodes.

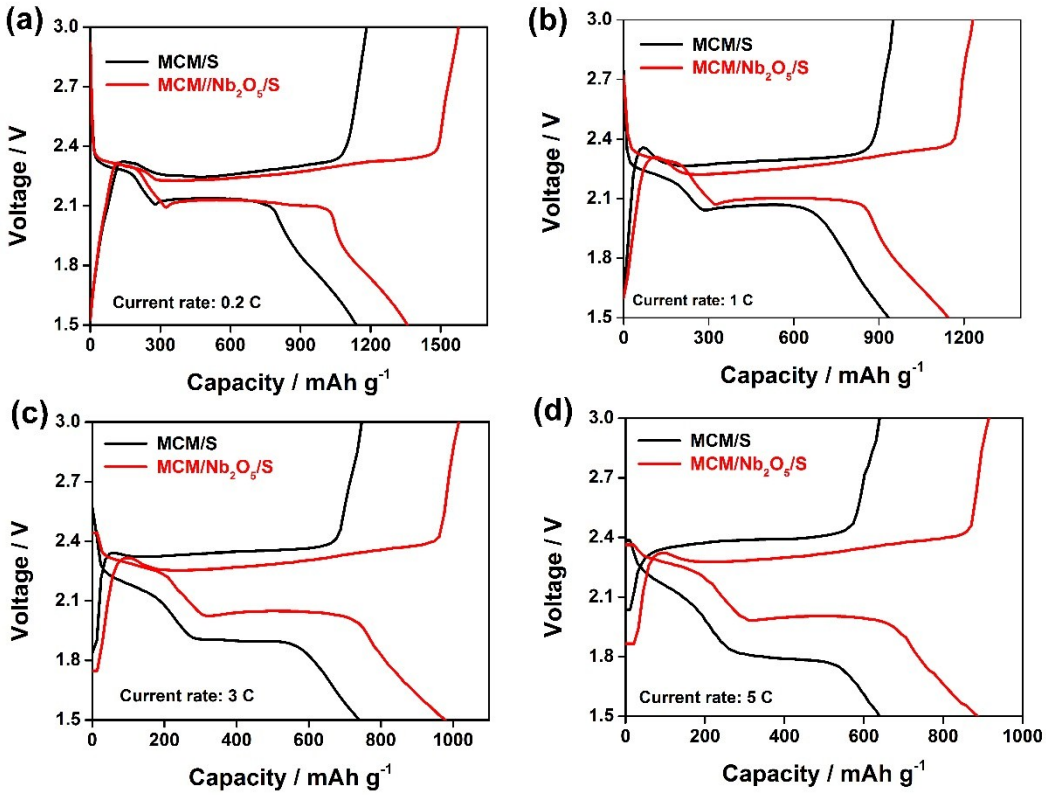

Figure S10. Discharge-charge profiles of two sulfur composites at varied current rates:

(a) 0.2 C. (b) 1 C. (c) 3 C. (d) 5 C.

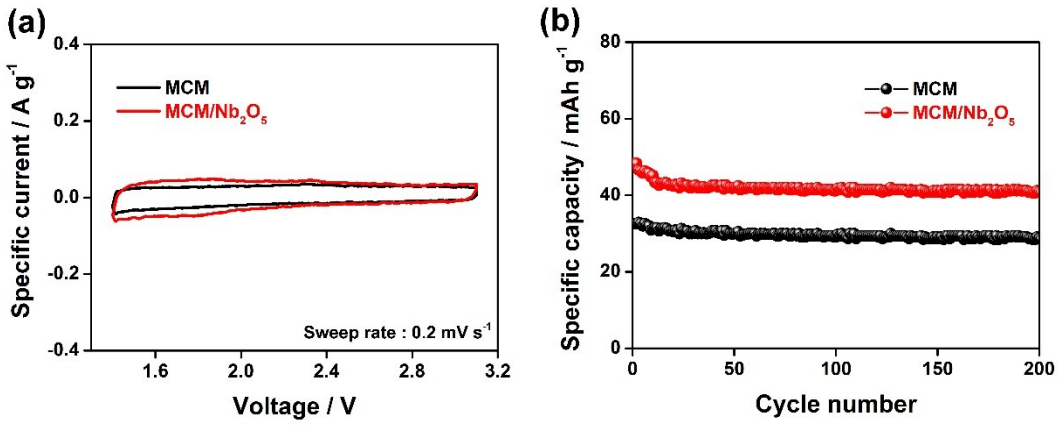

Figure S11. (a) CV curves at 0.2 mV s^{-1} and (b) long-term cycling performance of the MCMs and MCM/Nb_2O_5 electrodes.

The maximum capacity that Nb_2O_5 nanoparticles was expected to contribute by their Li^+ intersection pseudo-capacitive behavior is calculated according to

The specific capacity of Nb_2O_5 ×(Nb_2O_5 / S ratio of the MCM/Nb_2O_5/S cathode)

For example,

The specific capacity of Nb_2O_5 = 150 mA h g^{-1},

Nb_2O_5 / S ratio of the MCM/Nb_2O_5/S cathode = (0.4×0.095) / 0.6 = 0.064,

The increased specific capacity of sulfur contributed by Nb_2O_5 in the MCM/Nb_2O_5/S cathode = 150×0.064 = 10 mA h g^{-1}

2. Supplementary Table

Table S1. The performance comparison of MCM/Nb_2O_5 with other high performance matrices used in lithium sulfur batteries.

Matrix	Rate performance	Cycle performance
C/Nb_2O_5[this work]	5C, 887 mAh g^{-1}	2C, 650 mAh g^{-1}, 500 cycles
C/MnO_2[3]	1C, 690 mAh g^{-1}	0.5C, 660 mAh g^{-1}, 300cycles
C/TiO_2[4]	4C, 833 mAh g^{-1}	1C, 918 mAh g^{-1}, 500 cycles
C/$Ni(OH)_2$[5]	5C, 195 mAh g^{-1}	0.2C, 1250 mAh g^{-1}, 500 cycles
C/La_2O_3[6]	5C, 475 mAh g^{-1}	1C, 799 mAh g^{-1}, 100cycles
C/CoS_2[7]	2C, 1003 mAh g^{-1}	2C, 320 mAh g^{-1}, 2000 cycles
C/Co[8]	5C, 565 mAh g^{-1}	1C, 625 mAh g^{-1}, 500 cycles
$Mg_{0.6}Ni_{0.4}O$[9]	1C, 445 mAh g^{-1}	0.1C, 1100 mAh g^{-1}, 100 cycles
Porous hollow carbon[10]	3C, 450 mAh g^{-1}	0.5C, 1071 mAh g^{-1}, 100 cycles
Meso-/micro-porous carbon[11]	2C, 605 mAh g^{-1}	0.5C, 837 mAh g^{-1}, 200 cycles
Graphene/graphene oxide[12]	5C, 599 mAh g^{-1}	1C, 775 mAh g^{-1}, 500 cycles
Carbon nanotube[13]	5C, 705 mAh g^{-1}	5C, 570 mAh g^{-1}, 200 cycles
MoO_2[14]	2C, 635 mAh g^{-1}	0.1C, 570 mAh g^{-1}, 250 cycles
SnO_2[15]	0.8C, 700 mAh g^{-1}	0.5C, 736.6 mAh g^{-1}, 50 cycles
Ti_4O_7[16]	2C, 850 mAh g^{-1}	2C, 595 mAh g^{-1}, 500 cycles

References

1 H. Lindström, S. Södergren, A. Solbrand, H. Rensmo, J. Hjelm, A. Hagfeldt and S. E. Lindquist, J. Phys. Chem. B, 1997, 101, 7717.

2 X. Tao, J. Wang, C. Liu, H. Wang, H. Yao, G. Zheng, Z. W. Seh, Q. Cai, W. Li, G. Zhou, C. Zu and Y. Cui, *Nat. Commun.*, 2016, 7, 11203.

3 Z. Li, J. Zhang and X. W. (D.) Lou, *Angew. Chem. Int. Ed.*, 2015, **54**, 12886.

4 M. Yu, J. Ma, H. Song, A. Wang, F. Tian, Y. Wang, H. Qiu and R. Wang, *Energy. Environ. Sci.*, 2016, **9**, 1495.

5 S. Moon, Y. H. Jung, W. K. Jung, D. S. Jung, J. W. Choi and D. K. Kim, *Adv. Mater.*, 2013, **25**, 6547.

6 F. Sun, J. Wang, D. Long, W. Qiao, L. Ling, C. Lv and R. Cai, *J. Mater. Chem. A*, 2013, **1**, 13283.

7 Z. Yuan, H. J. Peng, T. Z. Hou, J. Q. Huang, C. M. Chen, D. W. Wang, X. B. Cheng, F. Wei and Q. Zhang, Nano Lett., 2016, **16**, 519.

8 Y. Li, J. M. Fan, M. S. Zheng and Q. F. Dong, *Energy. Environ. Sci.*, 2016. DOI: 10.1039/C6EE00104a

9 Y. Zhang, Y. Zhao, A. Yermukhambetova, Z. Bakenov and P. Chen, *J. Mater. Chem. A*, 2013, **1**, 295.

10 N. Jayaprakash, J. Shen, Surya S. Moganty, A. Corona and Lynden A. Archer *Angew. Chem. Int. Edit*., 2011, **123**, 6026.

11 Z. Li, Y. Jiang, L. Yuan, Z. Yi, C. Wu, Y. Liu, P. Strasser and Y. Huang, *ACS nano*, 2014, **8**, 9295.

12 W. Ahn, M. H. Seo, Y. S. Jun, D. U. Lee, F. M. Hassan, X. Wang, A. Yu and Z. Chen, ACS *Appl. Mater. Inter.*,2016, **8**, 1984.

13 Y. C. Jeong, K. Lee, T. Kim, J. H. Kim, J. Park, Y. S. a, S. J. Yang and C. R. Park, *J. Mate. Chem. A*, 2016, **4**, 819.

14 Q. Qu, T. Gao, H. Zheng, Y. Wang, X. Li, X. Li, J. Chen, Y. Han, J. Shao and H. Zheng, *Adv. Mater. Interfaces*, 2015, **2**, 1500048.

15 L. P. Zhang, Y. F. Wang, S. Q. Gou and J. H. Zeng, *J. Phys. Chem. C*, 2015, **119**, 28721.

16 Q. Pang, D. Kundu, M. Cuisinier and L. F. Nazar, *Nat. Commun.*, 2014, **5**, 4759.